Influence of atmospheric conditions on the role of trifluoroacetic acid in atmospheric sulfuric acid-dimethylamine nucleation

Ling Liu[1], Fangqun Yu[2], Kaipeng Tu[1], Zhi Yang[1], and Xiuhui Zhang[1]

[1]Key Laboratory of Cluster Science, Ministry of Education of China, School of Chemistry and Chemical Engineering, Beijing Institute of Technology, Beijing 100081, China
[2]Atmospheric Sciences Research Center, University at Albany, Albany, New York 12203, USA

Correspondence: Xiuhui Zhang (zhangxiuhui@bit.edu.cn)

Abstract. Ambient measurements combined with theoretical simulations have shown evidence that the tropospheric degradation end-products of Freon alternatives, trifluoroacetic acid (TFA), one of the most important and abundant atmospheric organic substances, can enhance the process of sulfuric acid (SA) - dimethylamine (DMA) - based nucleation process in urban environments. However, TFA is widespread all over the world with different atmospheric conditions, such as temperature and nucleation precursor concentration, which are the most important factors potentially influencing the atmospheric nucleation process and thus inducing different nucleation mechanisms. Herein, using the Density Functional Theory combined with the Atmospheric Cluster Dynamics Code, the influence of temperature and nucleation precursor concentrations on the role of TFA in the SA-DMA nucleation has been investigated. The results indicate that the growth trends of clusters involving TFA can increase with the decrease of temperature. The enhancement of particle formation rate by TFA and the contributions of SA-DMA-TFA cluster to the cluster formation pathways can be up to as much as 227 times and 95%, respectively, at relatively low temperature, low SA concentration, high TFA concentration, and high DMA concentration, such as in winter or at relatively high atmospheric boundary layer and in megacities far away from industrial sources of sulfur-containing pollutants. These results provide the perspective of the realistic role of TFA in different atmospheric environments, revealing the potential influence of the tropospheric degradation of Freon alternatives under a wide range of atmospheric conditions.

1 Introduction

Atmospheric aerosols have significant adverse impacts on climate and human health (Kulmala et al., 2007; Stevens and Feingold, 2009). New particle formation (NPF) is not only the key process of the formation of atmospheric aerosol but also the source of over half of the atmospheric cloud condensation nuclei, thus influencing cloud properties and Earth's energy balance (Bianchi et al., 2016; Merikanto et al., 2009). Especially, nucleation is the initial critical step of NPF. Well understanding the nucleation mechanisms and compositions of nucleation precursors can help to predict the impacts of NPF events and further provide theoretical clues to reducing the severe atmospheric aerosol pollution, haze. Sulfuric acid has been well recognized as the key nucleation precursor (Kulmala et al., 2013). Although sulfuric acid (SA) - dimethylamine (DMA) nucleation mechanism has been identified in the urban city of Shanghai, China (Yao et al., 2018), the nucleation mechanisms are not fully

understood and species contributing to NPF under different environments remain to be studied. Thus, other possible species
25 that may potentially enhance the NPF rates and the corresponding nucleation mechanism should be further explored.

Perfluorocarboxylic acids (PFCAs), widely distributed in the environment, can be formed from the oxidation of anthro-pogenically produced hydrofluorocarbons (HFCs), hydrochlorofluorocarbons (HCFCs) and hydrofluoro-olefins (HFOs) (Burkholder et al., 2015; Kazil et al., 2014; Pickard et al., 2018). Due to the worldwide distribution, chemical stability, and potential bi-ological toxicity, PFCAs are generally believed to be an important class of environmental contaminants present in various
30 environments. As the simplest and most abundant perfluorocarboxylic acid in the atmosphere (Tian et al., 2018), trifluoroacetic acid (TFA) is the pivotal product of the oxidative degradation processes of the Freon alternatives emitted from human activities (Madronich et al., 2015; Tromp et al., 1995). The concentration of TFA is relatively high in regions with scant rainfall because precipitation is the only predominant environmental sink of TFA (Ellis et al., 2001). Thus, the continuous production of TFA from the degradation of Freon alternatives combined with the lack of rainfall in some areas is more likely to induce the accu-
35 mulation of TFA. Recent ambient measurements and theoretical simulations have shown evidence for the participation of TFA in the formation of SA-DMA-based clusters under certain atmospheric conditions in urban Shanghai, China (Lu et al., 2020). The participation of TFA in NPF events can increase the number concentration of atmospheric aerosol particles and further potentially have effects on climate and human health.

The previous study on the role of TFA in SA-DMA-based NPF process is under the local atmospheric temperature and
40 nucleation precursor concentrations of Shanghai (Lu et al., 2020). Whereas TFA is widely distributed all over the world with different atmospheric conditions, among which temperature and concentrations of nucleation precursors are key influential factors in the nucleation process. Temperature can change with the variations of seasons, altitudes and climates, and nucleation precursor concentrations can vary with distances to the corresponding sources and altitudes. For example, DMA concentration is relatively high in polluted regions near its industrial, residential, or agricultural sources, but it is relatively low in the clean
45 and upper troposphere due to its short lifetime in the atmosphere. SA concentration is relatively high in areas near coal-fired power plant or industry, but it is relatively low in the areas far away from the emission sources of sulfur-containing pollutants. Besides, although TFA is widely distributed around the world, its concentration is relatively high in regions with scant rainfall. Therefore, it is important to elucidate the role of TFA in the NPF events under broad atmospheric conditions to understand the effect of TFA on the atmospheric environment systematically. In the present study, the influence of the varying
50 temperatures and precursor concentrations on the role of TFA in the SA-DMA-based clustering process was studied using Density Functional Theory combined with the Atmospheric Cluster Dynamic Code (ACDC) (McGrath et al., 2012; Olenius et al., 2013). The studied clusters are $(\text{Acid})_m \cdot (\text{Base})_n$, where $0 \leq n \leq m \leq 3$, in which acid molecules are TFA or/and SA and base molecule is DMA.

2 Methods

55 The M06-2X functional has been successfully used to describe noncovalent interaction (Elm et al., 2012; Zhao and Truh-lar, 2008) and estimate thermochemistry, equilibrium structures of atmospheric clusters (Bork et al., 2014; Elm et al., 2012,

2013). Furthermore, the 6-311++G(3df,3pd) basis set was chosen based on its excellent performance to estimate the properties of atmospheric relevant clusters when used in conjunction with the M06-2X functional (Herb et al., 2011, 2013; Nadykto et al., 2011, 2009). The single-point electronic energies were corrected using RI-CC2 method and aug-cc-pV(T+d)Z basis set

60 performed with the TURBOMOLE program, because of the good agreement between the simulated results based on the single-point electronic energies at RI-CC2/aug-cc-pV(T+d)Z level of theory and the experimental or field measurements (Kürten et al., 2018; Lu et al., 2020). Structures and the thermodynamic data of the presently studied clusters at 280 K are taken from previous studies (Lu et al., 2020).

The Atmospheric Cluster Dynamics Code (ACDC) (McGrath et al., 2012; Olenius et al., 2013) was used to simulate the

65 cluster formation process with the thermodynamic data generated by quantum chemistry calculations as input. Time development of the concentration of each cluster was solved by integrating numerically the birth-death equation (Kulmala et al., 2001) using the ode15s solver in MATLAB-R2013a program (Shampine and Reichelt, 1997).

The birth-death equation can be written as following Eq. (1):

$$\frac{dc_i}{dt} = \frac{1}{2}\Sigma_{j<i}\beta_{j,(i-j)}c_jc_{(i-j)} + \Sigma_j\gamma_{(i+j)\to i}c_{i+j} - \Sigma_j\beta_{i,j}c_ic_j - \frac{1}{2}\Sigma_{j<i}\gamma_{i\to j}c_i + Q_i - S_i \tag{1}$$

70 where c_i is the concentration of cluster i, $\beta_{i,j}$ is the collision coefficient between clusters i and j, $\gamma_{i\to j}$ is the γ evaporation coefficient of a molecule or a smaller cluster j from cluster i, Q_i is an outside source term of cluster i, and S_i is other possible sink term of cluster i.

The collision rate coefficients $\beta_{i,j}$ between clusters i and j were calculated as hard-sphere collision (Chapman et al., 1990) in Eq. (2):

75 $$\beta_{i,j} = \pi\left(r_i + r_j\right)^2\sqrt{\frac{8k_BT}{\pi\mu}} \tag{2}$$

where r_i is the radius of cluster i given by Multiwfn 3.3.8 program (Lu and Chen, 2012), k_B is the Boltzmann constant, T is the temperature and $\mu = m_im_j/(m_i + m_j)$ is the reduced mass. The cluster radius is half of the sum of the distance between the center of most distant atoms in cluster given by the Multiwfn 3.3.8 program (Lu and Chen, 2012) and the Van der Walls radii of these atoms.

80 Evaporation coefficients, $\gamma_{i\to j}$, were obtained from the corresponding collision coefficients and ΔG of clusters as shown in Eq. (3):

$$\gamma_{(i+j)\to i} = \beta_{i,j}\frac{P_{ref}}{k_BT}\exp\left(\frac{\Delta G_{i+j} - \Delta G_i - \Delta G_j}{k_BT}\right) \tag{3}$$

where P_{ref} is the reference pressure (in this case 1 atm) where the formation free energies were calculated and ΔG_i is the Gibbs free energy of formation of cluster i from monomers.

3 Results and Discussion

3.1 Influence of temperature and nucleation precursor concentrations on cluster stability and growth trend of clusters

The cluster stability is of great significance for the process of NPF. Atmospheric temperatures can vary with different seasons, altitudes, and climates. The temperature variation may have a significant influence on the aerosol cluster stability. Thermodynamically, Gibbs free energies of formation (ΔG) for clusters at different temperatures (280 K and 260 K) within the temperature range of the atmospheric boundary layer are shown in Table S1 in the Supplement. It shows that the ΔG decreases with the decrease of temperature, which reflects that clusters are more thermodynamically stable at relatively lower temperatures.

Kinetically, if the collision frequency ($\beta \cdot C$, β is shown in Table S2 in the Supplement) of a cluster with monomer molecule at the concentration of C is higher than its total evaporation frequency ($\Sigma \gamma$, Table S3 in the Supplement), this cluster can be considered to have the potential to continue growing. Thus, in order to analyze the growth trends of clusters involving TFA, ratios ($\beta \cdot C/\Sigma \gamma$) for collision frequencies with nucleation monomers versus total evaporation frequencies have been investigated (Table S4 in the Supplement). Here we take the ratio of $\beta \cdot C/\Sigma \gamma$ for clusters involving one TFA molecule at different temperatures as an example shown in Fig. 1 to study the growth trend of clusters. The $\beta \cdot C/\Sigma \gamma$ increases with the decrease of temperature (Fig. 1 and Table S4 in the Supplement), which indicates that it is easier for these clusters to grow at lower temperatures. The reason for this is that the influence of temperature variation on the evaporation coefficients (γ, where the temperature dependence is exponential (McGrath et al., 2012) is much greater than that on collision coefficients (β, where the dependence is in the square root of the temperature (McGrath et al., 2012)). At relatively low concentration of SA monomer, the ratios of $\beta \cdot C/\Sigma \gamma$ for $(SA)_1 \cdot (DMA)_2 \cdot (TFA)_1$ and $(SA)_2 \cdot (DMA)_3 \cdot (TFA)_1$ clusters are all larger than 1.0 at different temperatures (Fig. 1), which means that these two kinds of clusters tend to grow to larger clusters at 280 K and 260 K. Besides, $\beta \cdot C/\Sigma \gamma$ will increase when the nucleation monomer concentration increases. Thus, the growth trend of clusters can also be relatively high at higher concentrations of nucleation monomers.
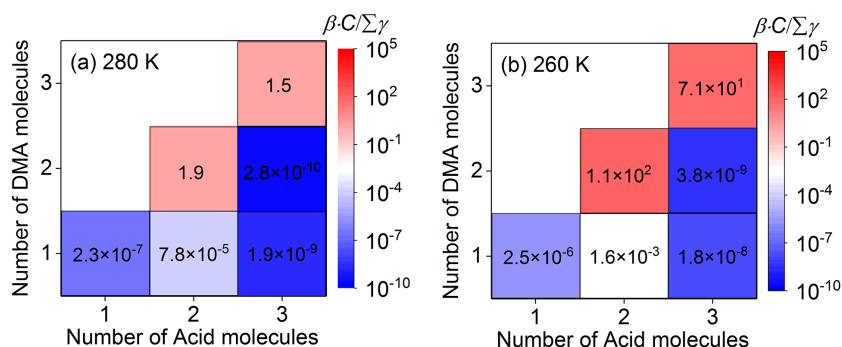
Figure 1. Ratios of SA monomer collision frequencies versus total evaporation frequencies ($\beta \cdot C/\Sigma \gamma$) for $(SA)_x \cdot (DMA)_y \cdot (TFA)_1$ ($0 \leq x \leq 2$, $1 \leq y \leq 3$, $y \leq x+1$) clusters at different temperatures (280 K and 260 K). Acid molecules are SA and TFA. $C = 1.0 \times 10^6$ molecules cm^{-3}.

3.2 Influence of temperature and nucleation precursor concentrations on particle formation rates

It can be seen that the stability and growth trend of clusters involving TFA vary with temperatures and concentrations of nucleation precursors from the above discussion. The stability and growth trend are closely related to particle formation rates. A study on the complicated influence of temperature and nucleation precursor concentration on particle formation rates becomes increasingly important to understand the realistic role of TFA in different atmospheric environments. Therefore, the potential influences of temperatures and concentrations of nucleation precursors on the particle formation rates of SA-DMA-TFA system have been investigated, as described below.

The temperature was obtained from the NASA Langley Research Center (LaRC) POWER Project funded through the NASA Earth Science/Applied Science Program (NASA, 2020). The studied temperature is the monthly average of temperature at 2 meters above the surface of the earth for a given month, averaged for that month over the 30 years (Jan. 1984 – Dec. 2013). The lifetime of TFA and SA are relatively long enough to ensure their atmospheric concentration to be in the present studied concentration range. However, because of the relatively short atmospheric lifetime of DMA concerning chemical reaction loss (Carl and Crowley, 1998; Qiu and Zhang, 2013), whether the concentration of DMA ([DMA]) can be relatively high or not remains to be determined. The global chemistry-transport model of GEOS-Chem (Yu and Luo, 2014) can predict the global [DMA], but the [DMA] may be underestimated possibly because of the underestimation about emissions and the regional average (Yu and Luo, 2014). Therefore, the cluster formation rates and the enhancements on cluster formation rate by TFA have been simulated at the [DMA] of 5 times the corresponding predicted [DMA] by the global chemistry-transport model of GEOS-Chem (Yu and Luo, 2014), taking four different typical cities with relatively high [DMA], such as Beijing, Shanghai, Los Angeles, and New Delhi, as an example (Fig. 2). The corresponding temperature and data of [DMA] are shown in Table S5 in the Supplement. The [SA] and [TFA] were chosen to be relatively low and high, 5.0×10^6 molecules cm^{-3} and 1.0×10^8 molecules cm^{-3} (Wu et al., 2014) respectively. The condensation sink (CS) is set to be 0.02 s^{-1}, which is the median of common CSs in the NPF events in the polluted areas (Yao et al., 2018).

As shown in Fig. 2, the enhancements on particle formation rate by TFA in the studied four cities are all higher than 1.0 in most of the months throughout the year, which indicates that TFA can enhance the SA-DMA particle formation rate in most of the year. The particle formation rate and enhancement on particle formation rate by TFA of Beijing are all higher than those of the other three studied cities in the corresponding month. This can be attributed to that the [DMA] and temperature in Beijing is relatively higher and lower than those of the other three studied cities, respectively. Besides, the particle formation rate and enhancement on particle formation rate by TFA are relatively high in spring and winter approximatively. This can be attributed to that temperature in spring and winter is relatively lower than other time all the year-round, respectively. Moreover, the enhancement on the particle formation rate by TFA is highest in Beijing among the studied four cities, which can be up to more than 13 times in January. Therefore, there is enough DMA in the realistic atmospheric boundary layer for TFA to enhance the SA-DMA nucleation process.

The influences of different atmospheric conditions on the effects of TFA in SA-DMA nucleation have been further studied in a wide range of common concentrations of nucleation precursors at the common temperatures (280 K and 260 K) in the
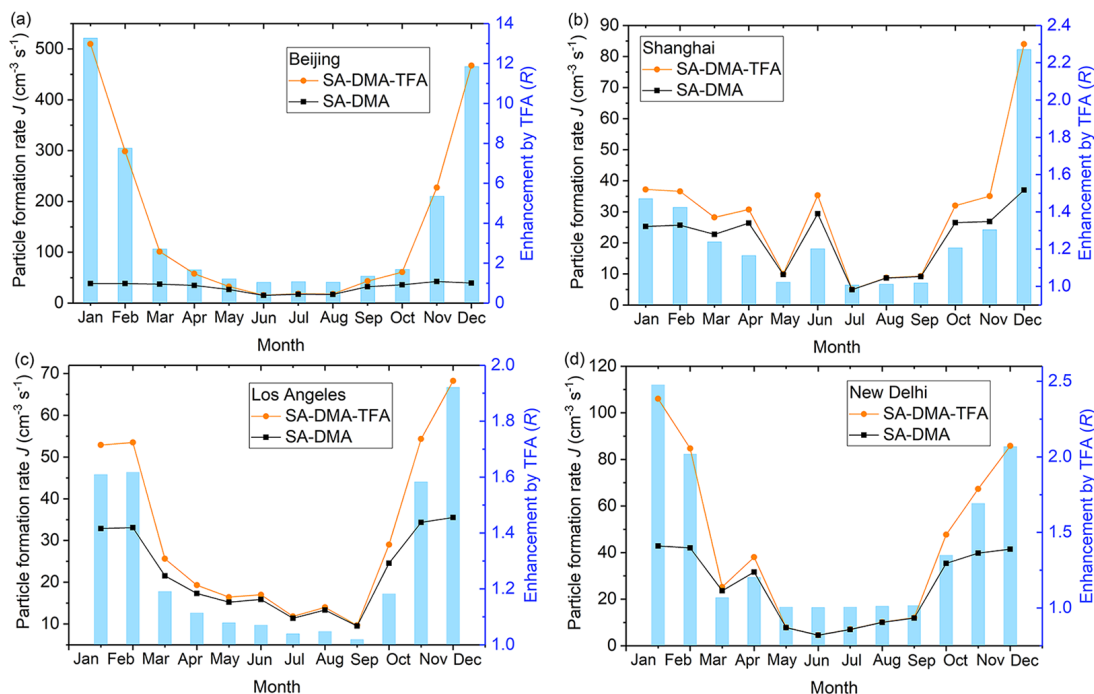
Figure 2. Particle formation rates (J, cm^{-3} s^{-1}) shown in orange circles (SA-DMA-TFA) and black squares (SA-DMA) and the enhancement on particle formation rates by TFA (R, $R = J_{\text{SA-DMA-TFA}}/J_{\text{SA-DMA}}$) shown in bar charts in (a) Beijing, (b) Shanghai, (c) Los Angeles, and (d) New Delhi.

atmospheric boundary layer (Fig. 3). The condensation sink (CS) in Fig. 3 is set to be 0.02 s^{-1}, which is the median of common CSs in the NPF events in the polluted areas (Yao et al., 2018). The results at other common CSs (0.01 s^{-1} and 0.03 s^{-1}) in the polluted atmosphere will be discussed below. DMA is one of the most common basic nucleation precursors in the atmosphere and can be released from industrial, residential, or agricultural sources (Mao et al., 2018). The common atmospheric concen-

145   trations of DMA monomer ([DMA]) are in the range of 1.0×10^7 to 1.0×10^9 molecules cm^{-3}. In this DMA concentration range, the particle formation rate and the enhancement of TFA on particle formation rate (R, $J_{\text{SA-DMA-TFA}}/J_{\text{SA-DMA}}$) have been studied at moderate atmospheric concentrations of SA ([SA]) and TFA ([TFA]). In general, the particle formation rate of SA-DMA-TFA system (Fig. 3 (a)) and the enhancement of particle formation rate by TFA (Fig. 3 (b)) increase with the decrease of temperature and increase with the increase of [DMA], which is in accordance with the negative dependence of the growth trend of clusters involving TFA on temperature and positive dependence on nucleation monomer concentration.

150   At [DMA] = 1.0×10^9 molecules cm^{-3} and 260 K, the particle formation rate of SA-DMA-TFA system can be up to more than 1200 cm^{-3} s^{-1}, and the corresponding enhancement of particle formation rate by TFA can nearly reach up to 2.2 times. Thus, the enhancement of particle formation rate by TFA is obvious in the regions with relatively low temperature and abundant DMA, such as in winter or at relatively high atmospheric boundary layer of industrial regions, megacities with a high

155   population density, or rural areas with animal housing and grazing regions (Mao et al., 2018).
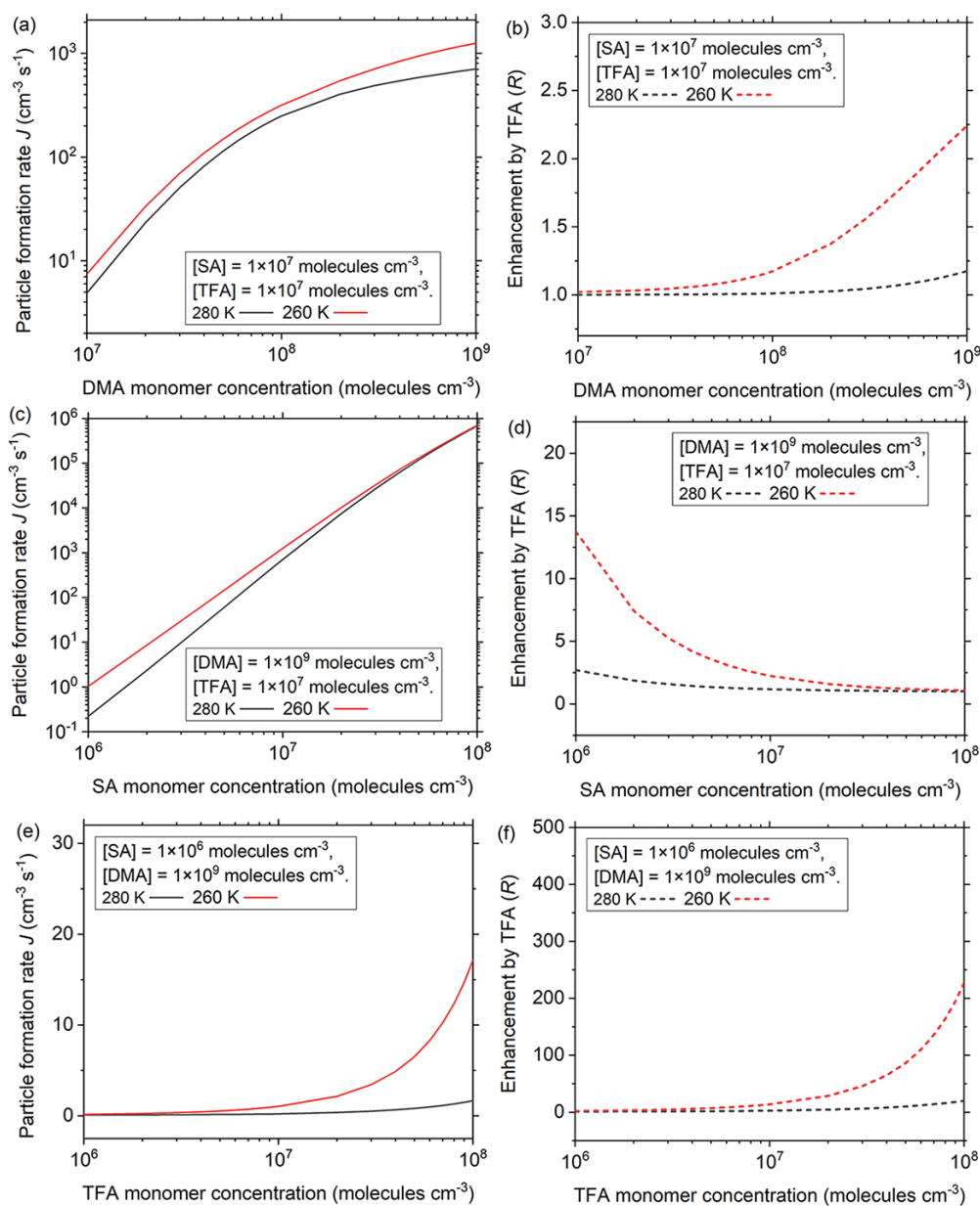
Figure 3. Particle formation rates (J, cm^{-3} s^{-1}) at different temperatures (280 K and 260 K) as a function of (a) DMA monomer concentrations, (c) SA monomer concentrations and (e) TFA monomer concentrations. Enhancement of particle formation rate by TFA (R, $R = J_{\text{SA}-\text{DMA}-\text{TFA}}/J_{\text{SA}-\text{DMA}}$) at different temperatures as a function of (b) DMA monomer concentrations, (d) SA monomer concentrations and (f) TFA monomer concentrations. Black and red lines are corresponding to 280 K and 260 K, respectively. CS = 0.02 s^{-1}.

In addition to the basic molecules, SA is the key acidic nucleation precursor in the atmosphere and its main source is coal-fired power plant and industry. The common atmospheric [SA] is in the range of 1.0×10^6 to 1.0×10^8 molecules cm^{-3} from clean areas to highly polluted areas (Kürten et al., 2012; Yao et al., 2018; Zheng et al., 2015). Given that the enhancement of TFA on particle formation rate is high at relatively high [DMA], the influence of [SA] on the role of TFA in NPF at [DMA] =

160 1.0×10^9 molecules cm^{-3} and different temperatures (280 K and 260 K) has been further studied. At different [SA], there are negative dependencies of particle formation rate and the enhancement of formation rate by TFA on temperature. At different temperatures, the particle formation rates all increase with the increase of [SA] (Fig. 3 (c)). However, the enhancement of particle formation rate by TFA increases with the decrease of [SA] and can be more than 14 times at relatively low [SA] (1.0×10^6 molecules cm^{-3}) at 260 K (Fig. 3 (d)). Thus, in addition to relatively high [DMA], the enhancement of particle

165 formation rate by TFA is obvious in the regions with relatively low temperature and low [SA], such as in winter or at relatively high atmospheric boundary layer of megacities and rural regions both far away from industrial sources of sulfur-containing pollutants, such as Beijing, China. Especially, with the effective regulations of emission reduction of the sulfur-containing pollutants, the atmospheric [SA] will decrease and the role of TFA (one of other important and potential acidic nucleation precursors except SA) in NPF will become increasingly important.

170 Furthermore, TFA is widely distributed in the atmosphere, especially in areas with scant rainfall. The variation of [TFA] may directly influence its role in the process of NPF. At relatively high [DMA] of 1.0×10^9 molecules cm^{-3} and relatively low [SA] of 1.0×10^6 molecules cm^{-3}, the influence of [TFA] on particle formation rate has been further studied at different temperatures (280 K and 260 K). Similar to the influence of temperature at different [DMA] or [SA], there are negative dependencies of the particle formation rate and the enhancement of particle formation rate by TFA on the temperature at different [TFA]. The

175 particle formation rate (Fig. 3 (e)) and the enhancement of TFA on particle formation rate increase (Fig. 3 (f)) with the increase of [TFA] at different temperatures, which is in accordance with the positive dependence of the growth trend for clusters on nucleation monomer concentration. At relatively high [TFA] (1.0×10^8 molecules cm^{-3}) and at a relatively low temperature of 260 K, the particle formation rate is more than 17 cm^{-3} s^{-1} and the corresponding enhancement of particle formation rate by TFA can be as high as more than 227 times. Therefore, the role of TFA is obvious in the regions with relatively low

180 temperatures and high [TFA], such as in winter or at relatively high atmospheric boundary layer and megacities or rural regions with scant rainfall far away from industrial sources of sulfur-containing pollutants.

Relatively high aerosol concentration can cause a large condensation sink (CS), thus scavenging newly formed molecular clusters (Yao et al., 2018). The CS can be different in different atmospheric environments. The particle formation rates and the corresponding enhancements by TFA at other common CSs (0.01 s^{-1} and 0.03 s^{-1}) in the polluted atmosphere are shown in

185 Figs. S1 and S2 in the Supplement, respectively. Although the particle formation rate and enhancement by TFA increase with the decrease of CS, the influence trend of temperature and nucleation precursor concentrations on them are the same.

3.3 Influence of temperature and precursor concentrations on the formation pathway of SA-DMA-TFA clusters

Variations of atmospheric conditions (temperature and concentration) can influence the particle formation rate of SA-DMA-TFA system as well as the corresponding enhancement by TFA. These trends of influence can be potentially explained by the

190 detailed SA-DMA-TFA cluster formation mechanism at the molecular level. Thus, the detailed cluster formation mechanisms of SA-DMA-TFA system under different temperatures and different concentrations of nucleation precursors have been further explored.

The cluster formation pathway at different concentrations of nucleation precursors (DMA, SA, and TFA) are first studied at the common temperature (280 K) of the atmospheric boundary layer (Fig. 4 (a)). The SA-DMA-TFA cluster formation path-
195 ways at different [DMA] have been shown at the moderate value of [SA] = 1.0×10^7 molecules cm^{-3} and [TFA] = 1.0×10^7 molecules cm^{-3}. There are two kinds of cluster formation pathways including the pure SA-DMA cluster formation and the SA-DMA-TFA cluster formation. The contributions of SA-DMA-TFA pathways (Fig. 4 (a-1)) increase with the increase of [DMA], which can explain why there is a positive dependence of SA-DMA-TFA particle formation rate on [DMA]. When [DMA] increases up to 1.0×10^9 molecules cm^{-3}, the cluster formation pathway involving TFA (blue arrows in Fig. 4 (a)) can
200 contribute to the cluster formation by up to 13% (4% + 9%). Therefore, there is a non-negligible contribution of clusters involving TFA to the particle formation pathway in regions with relatively high [DMA], such as regions near industrial, residential, or agricultural sources.

The SA-DMA-TFA cluster formation pathways at different [SA] have been studied at the relatively high [DMA] (1.0×10^9 molecules cm^{-3}) in view of that the contribution of TFA to the cluster formation pathway can be relatively high at high [DMA]
205 shown by the above results. The moderate value of [TFA] (1.0×10^7 molecules cm^{-3}) and common temperature (280 K) of the atmospheric boundary layer were chosen. The contributions of pathways at different [SA] (Fig. 4 (a-2)) are different. As shown in Fig. 4 (a-2), the contributions of branch pathways involving TFA increase with the decrease of [SA], which can be up to 61% (41% + 20%) at [SA] = 1.0×10^6 molecules cm^{-3}. Additionally, the cluster formation pathways with the variations of [TFA] at relatively low [SA] (1.0×10^6 molecules cm^{-3}) and relatively high [DMA] (1.0×10^9 molecules cm^{-3}) are also
210 shown in Fig. 4 (a-3). As expected, the contribution of pathways involving TFA to the cluster formation pathway is positively dependent on [TFA]. Especially, this contribution can be up to 93% at relatively low [SA], high [DMA], and high [TFA] (Fig. 4 (a-3)), which indicates that the cluster formation pathway involving TFA can dominate in megacities with scant rainfall far away from industrial sources of sulfur-containing pollutants. These variation trends of contributions of SA-DMA-TFA pathway are in accordance with the above discussion that there are a negative dependence and a positive dependence of SA-DMA-TFA
215 particle formation rate on [SA] and [TFA], respectively.

The SA-DMA-TFA cluster formation pathways at relatively low [SA], high [DMA], and high [TFA] are further studied at 260 K (Fig. 4 (b)). Compared to the cluster formation pathway at 280 K, additional pathways shown in blue arrows are present at 260 K. In addition to the two independent pathways of pure SA-DMA pathway and SA-DMA-TFA pathway starting from $(SA)_1 \cdot (DMA)_1$ cluster, $(SA)_2 \cdot (DMA)_2 \cdot (TFA)_1$ cluster can contribute to the formation of $(SA)_2 \cdot (DMA)_2$ cluster by the
220 evaporation of one TFA molecule. The contributions of the cluster formation pathway involving TFA can be up to 95% (18% + 77%). Therefore, the participation of TFA in the cluster formation process is extensive at the relatively low temperatures, such as in winter or at relatively high atmospheric boundary layer, which is in accordance with the negative dependence of SA-DMA-TFA cluster formation rates on temperature.
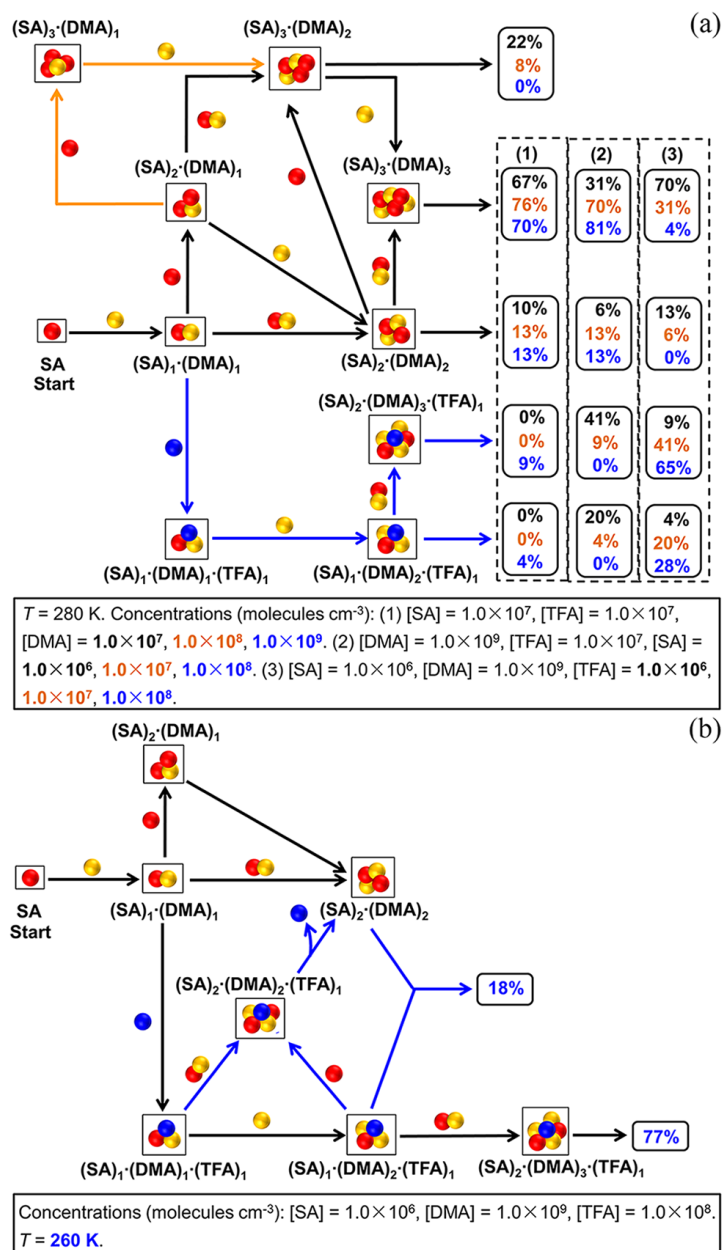
Figure 4. (a) Main cluster formation pathways of SA-DMA-TFA clusters at different [DMA], [SA] and [TFA]. The values of contribution shown in the right frames in black, orange and blue are corresponding to the contributions at (1) [DMA] of 1.0×10^7 molecules cm^{-3}, 1.0×10^8 molecules cm^{-3} and 1.0×10^9 molecules cm^{-3}, respectively, (2) [SA] of 1.0×10^6 molecules cm^{-3}, 1.0×10^7 molecules cm^{-3} and 1.0×10^8 molecules cm^{-3}, respectively, and (3) [TFA] of 1.0×10^6 molecules cm^{-3}, 1.0×10^7 molecules cm^{-3} and 1.0×10^8 molecules cm^{-3}, respectively. Black arrows show the common pathways present at all the studied [DMA]. Orange and blue arrows show the additional pathways present at [DMA] = 1.0×10^7 molecules cm^{-3} and [DMA] = 1.0×10^9 molecules cm^{-3}. (b) Main cluster formation pathways of SA-DMA-TFA clusters at 260 K. Black arrows show the common pathways present at both 260 K and 280 K. Blue arrows show the additional pathways present at 260 K compared with 280 K.

4 Atmospheric implications and conclusions

225 The present study shows that the influence of atmospheric conditions on the role of TFA in SA-DMA nucleation by the combination of high-level quantum-chemical calculations with the atmospheric cluster dynamic code (ACDC) simulations in the typical ranges of atmospheric temperature and nucleation precursor concentration. Results show a negative dependence of the growth trend of clusters involving TFA on temperature and a positive dependence on nucleation precursor concentration. The enhancement of particle formation rate by TFA and the contributions of SA-DMA-TFA cluster formation pathway to the

230 main cluster pathways increase with the decrease of temperature, the increase of [DMA] and [TFA], and decrease of [SA]. At [DMA] = 1.0×10^9 molecules cm^{-3}, [TFA] = 1.0×10^8 molecules cm^{-3}, [SA] = 1.0×10^6 molecules cm^{-3} and 260 K, the enhancement of SA-DMA particle formation rate by TFA can be as much as 227 times with the particle formation rate being more than 17 cm^{-3} s^{-1}. Under these atmospheric conditions, the corresponding contribution of clusters involving TFA in the cluster formation pathway is about 95% at 260 K. Therefore, the role of TFA in atmospheric aerosol nucleation is of great

235 significance in regions with relatively low temperature, high [DMA], and [TFA], and low [SA], such as cold megacities with scant rainfall. Especially, with the effective regulations of emission reduction of sulfur-containing pollutants, the enhancement of TFA on NPF becomes increasingly important. Under these atmospheric conditions, TFA can extensively participate in SA-DMA-based cluster formation process and further significantly enhance the particle formation rate, which can potentially enhance the number concentrations of cloud condensation nuclei and further influence the climate. Furthermore, this study

240 inspires on the potential underlying influence of the usage of Freon alternatives on air quality and global climate under different atmospheric conditions.

Data availability.   The data in this article are available from the corresponding author upon request (zhangxiuhui@bit.edu.cn)

Author contributions.   LL and XHZ designed the research. LL and KKT conducted the quantum chemistry calculations and the simulation by Atmospheric Cluster Dynamic Code. FQY conducted the simulation by global chemistry-transport model of GEOS-Chem. LL analyzed

245 data with the contributions from XHZ, FQY and ZY. LL and XHZ wrote the paper with contributions from all of the other co-authors.

Competing interests.   The authors declare that they have no conflict of interest.

Acknowledgements.   This work was supported by the National Natural Science Foundation of China (21976015, 21673175) and the China Postdoctoral Science Foundation (2020M680013). We thank the useful help of Theo Kurtén (University of Helsinki) and Hanna Vehkamäki (University of Helsinki). We acknowledge National Supercomputing Center in Shenzhen for providing the computational resources and

250 Turbomole.

References

Bianchi, F., Tröstl, J., Junninen, H., Frege, C., Henne, S., Hoyle, C. R., Molteni, U., Herrmann, E., Adamov, A., Bukowiecki, N., Chen, X., Duplissy, J., M., G., Hutterli, M., Kangasluoma, J., Kontkanen, J., Kürten, A., Manninen, H. E., Münch, S., Peräkylä, O., Petäjä, T., Rondo, L., Williamson, C., Weingartner, E., Curtius, J., Worsnop, D. R., Kulmala, M., Dommen, J., and Baltensperger, U.: New particle formation in the free troposphere: A question of chemistry and timing, Science, 352, 1109–1112, https://doi.org/10.1126/science.aad5456, 2016.

Bork, N., Elm, J., Olenius, T., and Vehkamäki, H.: Methane sulfonic acid-enhanced formation of molecular clusters of sulfuric acid and dimethyl amine, Atmos. Chem. Phys, 14, 12 023–12 030, https://doi.org/10.1080/10807039991289644, 2014.

Burkholder, J. B., Cox, R. A., and Ravishankara, A. R.: Atmospheric degradation of ozone depleting substances, their substitutes, and related species, Chem. Rev., 115, 3704–3759, https://doi.org/10.1021/cr5006759, 2015.

Carl, S. A. and Crowley, J. N.: Sequential two (blue) photon absorption by NO_2 in the presence of H_2 as a source of OH in pulsed photolysis kinetic studies: Rate constants for reaction of OH with CH_3NH_2,$(CH_3)_2NH$,$(CH_3)_3N$, and $C_2H_5NH_2$ at 295 K, J. Phys. Chem. A, 102, 8131–8141, https://doi.org/10.1021/jp9821937, 1998.

Chapman, S., Cowling, T. G., and Burnett, D.: The mathematical theory of non-uniform gases: an account of the kinetic theory of viscosity, thermal conduction and diffusion in gases, Cambridge university press, 1990.

Ellis, D. A., Hanson, M. L., Sibley, P. K., Shahid, T., Fineberg, N. A., Solomon, K. R., Muir, D. C. G., and Mabury, S. A.: The fate and persistence of trifluoroacetic and chloroacetic acids in pond waters, Chemosphere, 42, 309–318, https://doi.org/10.1016/S0045-6535(00)00066-7, 2001.

Elm, J., Bilde, M., and Mikkelsen, K. V.: Assessment of density functional theory in predicting structures and free energies of reaction of atmospheric prenucleation clusters, J. Chem. Theory. Comput., 8, 2071–2077, https://doi.org/10.1039/c3cp52616j, 2012.

Elm, J., Merete, B., and Mikkelsen, K. V.: Assessment of binding energies of atmospherically relevant clusters, Phys. Chem. Chem. Phys., 15, 16 442–16 445, https://doi.org/10.1039/c3cp52616j, 2013.

Herb, J., Nadykto, A. B., and Yu, F.: Large ternary hydrogen-bonded pre-nucleation clusters in the Earth's atmosphere, Chem. Phys. Lett., 518, 7–14, https://doi.org/10.1016/j.cplett.2011.10.035, 2011.

Herb, J., Xu, Y., Yu, F., and Nadykto, A. B.: Large hydrogen-bonded pre-nucleation $(HSO_4{}^-)(H_2SO_4)_m(H_2O)_k$ and $(HSO_4{}^-)(NH_3)(H_2SO_4)_m(H_2O)_k$ clusters in the Earth's atmosphere, J. Phys. Chem. A, 117, 133–152, https://doi.org/10.1021/jp3088435, 2013.

Kazil, J., McKeen, S., Kim, S.-W., Ahmadov, R., Grell, G. A., Talukdar, R. K., and Ravishankara, A. R.: Deposition and rainwater concentrations of trifluoroacetic acid in the United States from the use of HFO-1234yf, J. Geophys. Res. Atmos., 119, 14–059, https://doi.org/10.1002/2014JD022058, 2014.

Kulmala, M., Maso, M. D., Mäkelä, J. M., Pirjola, L., Väkevä, M., Aalto, P., Miikkulainen, P., Hämeri, K., and O'dowd, C. D.: On the formation, growth and composition of nucleation mode particles, Tellus B, 53, 479–490, https://doi.org/10.3402/tellusb.v53i4.16622, 2001.

Kulmala, M., Riipinen, I., Sipilä, M., Manninen, H. E., Petäjä, T., Junninen, H., Dal Maso, M., Mordas, G., Mirme, A., Vana, M., Hirsikko, A., Laakso, L., Harrison, R. M., Hanson, I., Leung, C., Lehtinen, K. E. J., and Veli-Matti, K.: Toward direct measurement of atmospheric nucleation, Science, 318, 89–92, https://doi.org/10.1126/science.1144124, 2007.

Kulmala, M., Kontkanen, J., Junninen, H., Lehtipalo, K., Manninen, H. E., Nieminen, T., Petäjä, T., Sipilä, M., Schobesberger, S., Rantala, P., Franchin, A., Jokinen, T., Järvinen, E., Äijälä, M., Kangasluoma, Juha adn Hakala, J., Aalto, P. P., Paasonen, P., Mikkilä, J., Vanhanen, J., Aalto, J., Hakola, H., Makkonen, U., Ruuskanen, T., Mauldin III, R. L., Duplissy, J., Vehkamäki, H., Bäck, J., Kortelainen, A., Riipinen, I., Kurtén, T., Johnston, M. V., Smith, J. N., Ehn, M., Mentel, T. F., Lehtinen, K. E. J., Laaksonen, A., Kerminen, V.-M., and Worsnop, D. R.: Direct observations of atmospheric aerosol nucleation, Science, 339, 943–946, https://doi.org/10.1126/science.1227385, 2013.

Kürten, A., Rondo, L., Ehrhart, S., and Curtius, J.: Calibration of a chemical ionization mass spectrometer for the measurement of gaseous sulfuric acid, J. Phys. Chem. A, 116, 6375–6386, https://doi.org/10.1021/jp212123n, 2012.

Kürten, A., Li, C., Bianchi, F., Curtius, J., Dias, A., Donahue, N. M., Duplissy, J., Flagan, R. C., Hakala, J., Jokinen, T., Kirkby, J., Kulmala, M., Laaksonen, A., Lehtipalo, K., Makhmutov, V., Onnela, A., Rissanen, M. P., Simon, M., Sipilä, M., Stozhkov, Y., Tröstl, J., Ye, P., and McMurry, P. H.: New particle formation in the sulfuric acid-dimethylamine-water system: reevaluation of CLOUD chamber measurements and comparison to an aerosol nucleation and growth model, Atmos. Chem. Phys., https://doi.org/10.5194/acp-18-845-2018, 2018.

Lu, T. and Chen, F.: Multiwfn: a multifunctional wavefunction analyzer, J Comput Chem, 33, 580–592, https://doi.org/10.1002/jcc.22885, 2012.

Lu, Y., Liu, L., Ning, A., Yang, G., Liu, Y., Kurtén, T., Vehkamäki, H., Zhang, X., and Wang, L.: Atmospheric sulfuric acid-dimethylamine nucleation enhanced by trifluoroacetic acid, Geophys. Res. Lett., 47, e2019GL085 627, https://doi.org/10.1029/2019gl085627, 2020.

Madronich, S., Shao, M., Wilson, S. R., Solomon, K. R., Longstreth, J. D., and Tang, X. Y.: Changes in air quality and tropospheric composition due to depletion of stratospheric ozone and interactions with changing climate: implications for human and environmental health, Photochem. Photobiol. Sci., 14, 149–169, https://doi.org/10.1039/c4pp90037e, 2015.

Mao, J., Yu, F., Zhang, Y., An, J., Wang, L., Zheng, J., Yao, L., Luo, G., Ma, W., Yu, Q., Huang, C., Li, L., and Chen, L.: High-resolution modeling of gaseous methylamines over a polluted region in China: source-dependent emissions and implications of spatial variations, Atmos. Chem. Phys., 18, 7933–7950, https://doi.org/10.5194/acp-18-7933-2018, 2018.

McGrath, M. J., Olenius, T., Ortega, I. K., Loukonen, V., Paasonen, P., Kurtén, T., Kulmala, M., and Vehkamäki, H.: Atmospheric Cluster Dynamics Code: a flexible method for solution of the birth-death equations, Atmos. Chem. Phys., 12, 2345–2355, https://doi.org/10.5194/acp-12-2345-2012, 2012.

Merikanto, J., Spracklen, D. V., Mann, G. W., Pickering, S. J., and Carslaw, K. S.: Impact of nucleation on global CCN, Atmos. Chem. Phys., 9, 8601–8616, https://doi.org/10.5194/acpd-9-12999-2009, 2009.

Nadykto, A., Yu, F., and Herb, J.: Ammonia in positively charged pre-nucleation clusters: a quantum-chemical study and atmospheric implications, Atmos. Chem. Phys., 9, https://doi.org/10.5194/acpd-9-4231-2009, 2009.

Nadykto, A. B., Yu, F., Jakovleva, M. V., Herb, J., and Xu, Y.: Amines in the Earth's atmosphere: a density functional theory study of the thermochemistry of pre-nucleation clusters, Entropy, 13, 554–569, https://doi.org/10.3390/e13020554, 2011.

NASA: NASA POWER Data Access Viewer, https://power.larc.nasa.gov/data-access-viewer/, last access: 1st June, 2020.

Olenius, T., O., K.-M., K., O. I., T., K., and H., V.: Free energy barrier in the growth of sulfuric acid-ammonia and sulfuric acid-dimethylamine clusters, J. Chem. Phys., 139, 084 312, https://doi.org/10.1063/1.4819024, 2013.

Pickard, H. M., Criscitiello, A. S., Spencer, C., Sharp, M. J., Muir, D. C. G., De Silva, A. O., and Young, C. J.: Continuous non-marine inputs of per-and polyfluoroalkyl substances to the High Arctic: a multi-decadal temporal record, Atmos. Chem. Phys., 18, 5045–5058, https://doi.org/10.5194/acp-18-5045-2018, 2018.

Qiu, C. and Zhang, R.: Multiphase chemistry of atmospheric amines, Phys. Chem. Chem. Phys., 15, 5738–5752, https://doi.org/10.1039/c3cp43446j, 2013.

325   Shampine, L. F. and Reichelt, M. W.: The matlab ode suite, SIAM J. Sci. Comput., 18, 1–22, https://doi.org/10.1137/S1064827594276424, 1997.

Stevens, B. and Feingold, G.: Untangling aerosol effects on clouds and precipitation in a buffered system, Nature, 461, 607–613, https://doi.org/10.1038/nature08281, 2009.

Tian, Y., Yao, Y., Chang, S., Zhao, Z., Zhao, Y., Yuan, X., Wu, F., and Sun, H.: Occurrence and phase distribution of neutral and ionizable
330   per-and polyfluoroalkyl substances (PFASs) in the atmosphere and plant leaves around landfills: a case study in Tianjin, China, Environ. Sci. Technol., 52, 1301–1310, https://doi.org/10.1021/acs.est.7b05385, 2018.

Tromp, T. K., Ko, M. K. W., Rodriguez, J. M., and Sze, N. D.: Potential accumulation of a CFC-replacement degradation product in seasonal wetlands, Nature, 376, 327–330, 1995.

Wu, J., Martin, J. W., Zhai, Z., Lu, K., Li, L., Fang, X., Jin, H., Hu, J., and Zhang, J.: Airborne trifluoroacetic acid and its fraction from the
335   degradation of HFC-134a in Beijing, China, Environ. Sci. Technol., 48, 3675–3681, https://doi.org/10.1021/es4050264, 2014.

Yao, L., Garmash, O., Bianchi, F., Zheng, J., Yan, C., Kontkanen, J., Junninen, H., Mazon, S. B., Ehn, M., Paasonen, P., Sipilä, M., Wang, M., Wang, X., Xiao, S., Chen, H., Lu, Y., Zhang, B., Wang, D., Fu, Q., Geng, F., Li, L., Wang, H., Qiao, L., Yang, X., Chen, J., Kerminen, V.-M., Petäjä, T., Worsnop, D. R., Kulmala, M., and Wang, L.: Atmospheric new particle formation from sulfuric acid and amines in a Chinese megacity, Science, 361, 278–281, https://doi.org/10.1126/science.aao4839, 2018.

340   Yu, F. and Luo, G.: Modeling of gaseous methylamines in the global atmosphere: impacts of oxidation and aerosol uptake, Atmos. Chem. Phys, 14, 12–455, https://doi.org/10.5194/acp-14-12455-2014, 2014.

Zhao, Y. and Truhlar, D. G.: The M06 suite of density functionals for main group thermochemistry, thermochemical kinetics, noncovalent interactions, excited states, and transition elements: two new functionals and systematic testing of four M06-class functionals and 12 other functionals, Theor. Chem. Account., 120, 215–241, https://doi.org/10.1007/s00214-007-0310-x, 2008.

345   Zheng, J., Yang, D., Ma, Y., Chen, M., Cheng, J., Li, S., and Wang, M.: Development of a new corona discharge based ion source for high resolution time-of-flight chemical ionization mass spectrometer to measure gaseous H_2SO_4 and aerosol sulfate, Atmos. Environ., 119, 167–173, https://doi.org/10.1016/j.atmosenv.2015.08.028, 2015.